Journal of Nuclear Materials 463 (2015) 471–476

Contents lists available at ScienceDirect

Journal of Nuclear Materials

journal homepage: www.elsevier.com/locate/jnucmat

Divertor plasma conditions and neutral dynamics in horizontal and vertical divertor configurations in JET-ILW low confinement mode plasmas

M. Groth [b,*,1], S. Brezinsek [c], P. Belo [d,e], M. Brix [e], G. Calabro [f], A. Chankin [g], M. Clever [c], J.W. Coenen [c], G. Corrigan [e], P. Drewelow [h], C. Guillemaut [i], D. Harting [e], A. Huber [c], S. Jachmich [j], A. Järvinen [b], U. Kruezi [e], K.D. Lawson [e], M. Lehnen [c,k], C.F. Maggi [g], C. Marchetto [l], S. Marsen [h], F. Maviglia [m], A.G. Meigs [e], D. Moulton [b], C. Silva [d], M.F. Stamp [e], S. Wiesen [c], The EFDA-JET Contributors [a,2]

[a] JET-EFDA, Culham Science Centre, OX14 3DB, Abingdon, UK
[b] Aalto University, Association EURATOM-Tekes, Otakaari 4, Espoo, Finland
[c] Forschungszentrum Jülich, IEK4 – Plasma Physik, Jülich, Germany
[d] Institute of Plasmas and Nuclear Fusion, Association EURATOM/IST, Lisbon, Portugal
[e] Culham Centre for Fusion Energy, Association EURATOM-CCFE, Abingdon, UK
[f] Association EURATOM-ENEA, Frascati, Italy
[g] Max-Planck Institute for Plasma Physics, EURATOM Association, Garching, Germany
[h] Max-Planck-Institute for Plasma Physics, EURATOM Association, Greifswald, Germany
[i] Association EURATOM CEA, CEA/DSM/IRFM, Cadarache, France
[j] Association 'Euratom-Belgian state', Ecole Royale Militaire, Brussels, Belgium
[k] ITER Organisation, 13115 Saint-Paul-Lez-Durance, France
[l] Association EURATOM-ENEA, IPP-CNR, Milan, Italy
[m] Association EURATOM-ENEA-CREATE, Napoli, Italy

ARTICLE INFO

Article history:
Available online 17 December 2014

ABSTRACT

Measurements of the plasma conditions at the low field side target plate in JET ITER-like wall ohmic and low confinement mode plasmas show minor differences in divertor plasma configurations with horizontally and vertically inclined targets. Both the reduction of the electron temperature in the vicinity of the strike points and the rollover of the ion current to the plates follow the same functional dependence on the density at the low field side midplane. Configurations with vertically inclined target plates, however, produce twice as high sub-divertor pressures for the same upstream density. Simulations with the EDGE2D-EIRENE code package predict significantly lower plasma temperatures at the low field side target in vertical than in horizontal target configurations. Including cross-field drifts and imposing a pumping by-pass leak at the low-field side plate can still not recover the experimental observations.

1. Introduction

The spatial distribution of deuterium neutrals (i.e., deuterium atoms and molecules) in the divertor chamber of tokamaks and their dynamics play a key role in achieving detached divertor conditions. Partial detachment of the divertor plasma at the strike zones is the mode of operation required in ITER to limit the heat fluxes to the divertor target plates below 10 MW/m^2 and to minimise erosion [1]. This is, in particular, important in tokamaks with tungsten plasma-facing components as tungsten sputtering is significantly reduced at plasma temperatures below 10 eV [2]. In tokamaks neutrals arise predominately from recycling of plasma ions at plasma-facing components. These neutrals re-ionise and charge-exchange with plasma ions, thereby dispersing heat and momentum. A fraction of neutrals leaks into the main chamber leading to both fuelling of the core plasma and power losses due to charge exchange with plasma ions. The divertor geometry, target inclination and plasma configuration are key parameters in confining neutrals within the divertor chamber. In particular, vertical target (VT) configurations in closed divertors have shown to better confine neutrals than horizontal configurations as recycling neutrals are preferentially released in the direction of the

* Corresponding author at: Aalto University, Otakaari 4, 02150 Espoo, Finland.
E-mail address: mathias.groth@aalto.fi (M. Groth).
[1] Presenting author.
[2] See App. of F. Romanelli et al., Proc. of the 24th IAEA Fusion Energy Conf. 2012, San Diego, USA.

http://dx.doi.org/10.1016/j.jnucmat.2014.12.030
0022-3115/

separatrix and private flux-region (PFR) [3–5]. Higher neutral densities in the divertor chamber also promote better pumping of deuterium, thus fuel density control, and helium ash removal. While there is a clear effect of the divertor neutral density distribution on divertor plasma configuration, its impact on the plasma conditions is more ambiguous. Measurements of the electron temperature, T_e, in Alcator C-mod showed a fivefold reduction of T_e at the low-field side (LFS) target plate in detached conditions when the LFS strike point is place on a vertically inclined surfaces compared to a horizontal (flat) surface [3]. Initial experiments in JET with the 1994–95 MkI pumped divertor showed a similar effect, in particular when the divertor strike zone was located on the lower end of the vertical target plate [5]. However, gas recirculation within the divertor structure produced a complicated ionisation pattern that masked some of the geometry effects.

In this contribution the effect of the divertor plasma configuration on the plasma conditions at the divertor target plates and the neutral pressure in the sub-divertor is re-visited in extensively characterised ohmic and neutral-beam heated, low-confinement (L-mode) discharges in the JET ITER-like wall configuration [6,7]. The JET ITER-like wall (ILW) comprises beryllium plasma-facing component in the main chamber, and tungsten in the divertor [8]. Key scrape-off layer (SOL) parameters, such as profiles of the ion currents, j_{sat}, to, and T_e along the high-field side (HFS) and LFS plates, and the sub-divertor pressure, $p_{sub\text{-}div}$, near the divertor cryogenic pump were measured for two different divertor plasma configurations (Fig. 1): a configuration with the LFS strike point placed in the centre of the load-bearing horizontal tile and a configuration with the LFS strike point on the lower part of the JET vertical divertor structure on the LFS (VT). In both configurations the HFS strike point was on the HFS vertical target plate. For simplicity and clarity of this paper, we refer to the former configuration as horizontal target (HT) configuration. The magnetic shapes in the main chamber were almost identical, including large gaps to the HFS and LFS wall (9.5 cm and 5.1 cm, respectively). To minimise the impact of plasma interaction with the top of the vacuum vessel, low triangularity configurations (of δ_u of approximately 0.2) were chosen (separatrix-top real space, 22 cm). The experiments were carried out at JET-typical pairs of plasma currents (I_p) and toroidal fields (B_T) were: (2.0 MA, 2.0 T) and (2.5 MA, 2.5 T) for the ohmic and neutral beam-heated L-mode plasma, respectively. These currents and fields resulted in an edge safety factor, q_{95}, of 3.4. The ion $\mathbf{B} \times \nabla B$ drift direction was into the divertor. The discharges were fuelled with deuterium gas from the top of the vacuum vessel, and from injection modules at the HFS and LFS of the divertor base plates (Fig. 1). In both HT and VT configurations the injection from the HFS divertor module was into the PFR, while the injection from the LFS module was either into the common SOL (HT) or into the PFR (VT). In both cases the selected injection modules are sufficiently close to the pumping plena in the lower corners of the divertor for some D_2 to reach the sub-divertor directly without processing through the divertor plasma. The divertor cryo pump located within the sub-divertor structure at the LFS (Fig. 1) was held at liquid nitrogen temperature to pump deuterium gas in this region. Both continuous fuelling to the density limit, and fuelling steps to establish constant plasma conditions for several seconds were performed. During the continuous fuelling scan, the strike point locations were held constant, while 2–3 cm strike point sweeps over the divertor Langmuir probes were executed to obtain the spatial profiles of j_{sat}, T_e and the electron density, n_e, along the target plates. A baratron was used to measure the pressure at the end of an approximately 3 m long tube below the cryo pump [9]. In addition to these key diagnostics, the plasma conditions upstream and the radiation profiles across the SOL were comprehensively characterised using the full suite of JET diagnostics. A comprehensive description of these plasmas and measurements is given in [7].

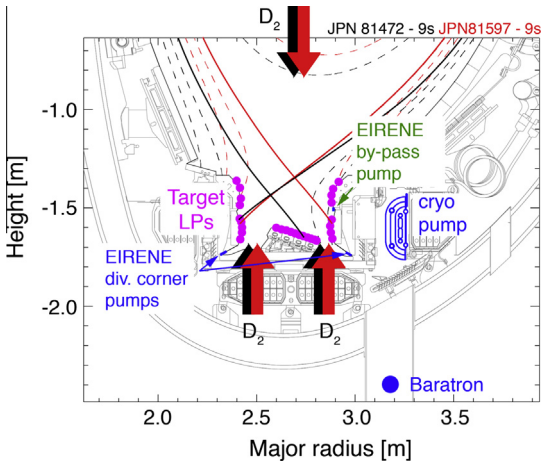

Fig. 1. JET divertor and sub-divertor structure, and the HT-horizontal (HT, black, JPN 81472) and vertical (VT, red, JPN 81597) divertor plasma configurations. The main features of the sub-divertor, the gas injection locations, and the primary divertor diagnostics are highlighted. The assumed pump locations in EIRENE are shown in blue for the divertor corners, and in green for a by-pass between two adjacent toroidal rows at the LFS vertical target. (For interpretation of the references to colour in this figure legend, the reader is referred to the web version of this article.)

The neutral Monte-Carlo code EIRENE [10] was used to predict the neutral dynamics of deuterium in the SOL in the HT and VT configurations. The code solves the kinetic Boltzmann equations for atomic and molecular hydrogen species in plasmas (electrons, hydrogen ions, and impurity ions). EIRENE is iteratively coupled with the edge fluid code EDGE2D [11,12], which solves the Bragiinski fluid equations in the parallel-**B** direction and assumes a diffusive-convective model in the radial direction. The radial transport coefficients for particles (here, diffusion only) and energy were determined by matching the measured radial profiles of n_e and T_e at the LFS midplane (see Fig. 9 of [7]). For deuterium-only cases, cross-field drifts due to $\mathbf{E} \times \mathbf{B}$ and $\mathbf{B} \times \nabla B$ [13] were included in the simulations. The (coupled) EDGE2D-EIRENE calculations were carried out on a non-orthogonal grid including the SOL and the pedestal region. The EIRENE grid utilises the EDGE2D grid and extends further to the actual main chamber and PFR walls (far SOL or halo region). For the halo region vacuum was assumed. To fully account for hydrogen ion-neutral and ion-molecular interaction at high divertor densities ($>10^{20}$ m^{-3}) the currently most complete EIRENE model [14] was used. Deuterium fuelling was simulated in EIRENE by injection from the EDGE2D outermost grid boundary in the PFR, and pumping by imposing albedos (of value 0.94) at two primary surfaces in the divertor corners on the EIRENE grid (Fig. 1). The albedo was derived in previous studies [12] and used as free parameter in these investigations. Following deuterium into the sub-divertor was not yet included, and thus the current to the pump surfaces used as a proxy to assess the impact of deuterium removal on the plasma solution. Pumping of neutrals at other surfaces was not imposed. Deuterons were fully recycled at the divertor targets and the outermost EDGE2D grid cells. Beryllium and tungsten were included in the simulations. Carbon was presently omitted due to limitations with the EDGE2D; however, the carbon content was measured at the level of 0.05%, or below, [15] justifying such simplification. Further details on the impurity model can be found in [7] and therein.

The primary outputs of the EDGE2D-EIRENE simulations used throughout this paper are the radiated power in the SOL and pedestal regions ($P_{rad,SOL+ped}$), the profiles j_{sat} and T_e at the target plates, the neutral currents to the pumping surfaces (I_{pump}), and

the leakage neutral currents from the divertor into the main chamber (I_{leak}). These parameters will be compared to the experimental equivalents where available.

2. Measurements of plasma and neutral conditions in the divertor

In ohmic and neutral beam-heated plasmas held at approximately constant heating power (Fig. 2a), the radiated power integrated over the SOL and pedestal regions increased nearly linearly with increasing electron density at the core plasma edge (Fig. 2b). Here, the line-averaged electron density across the outer edge at the LFS of the core plasma, $<n_e>_{l,edge}$, is used as the independent parameter. Within the data set shown for the neutral beam-heated plasmas, $P_{rad,SOL+ped}$ tripled from going to low-recycling to fully detached plasmas in the HT configuration. When integrated over the SOL and pedestal region, there is no difference in $P_{rad,SOL+ped}$ between the HT and VT configurations. (At the writing of this report there no data available for fully detached plasmas in the VT configuration.) The same trend and increase in $P_{rad,SOL+ped}$, and its independence on divertor plasma configuration was observed in ohmic plasmas [6].

The peak T_e in the immediate vicinity of the separatrix at the LFS plate, $T_{e,LFS,pk}$, monotonically decreased from about 30 to 40 eV at the lowest $\langle n_e\rangle_{l,edge}$ to 20 eV at mid-range $\langle n_e\rangle_{l,edge}$, and decreased steeply from 20 eV to less then 10 eV as $\langle n_e\rangle_{l,edge}$ was raised further (Fig. 2c). At the highest $\langle n_e\rangle_{l,edge}$ in the HT configuration $T_{e,LFS,pk}$ was measured (with the probes) at 4 eV. High-n Balmer line analysis would suggest temperatures below 1 eV [16]. At the HFS plate $T_{e,pk}$ was observed at or below 10 eV over the entire $\langle n_e\rangle_{l,edge}$ range investigated, indicating significantly cooler plasma conditions within the HFS divertor plasma. This observation is consistent with many similar studies in other tokamaks in configurations with the ion $\mathbf{B}\times\nabla B$ drift direction into the divertor (Ref. [17] and therein).

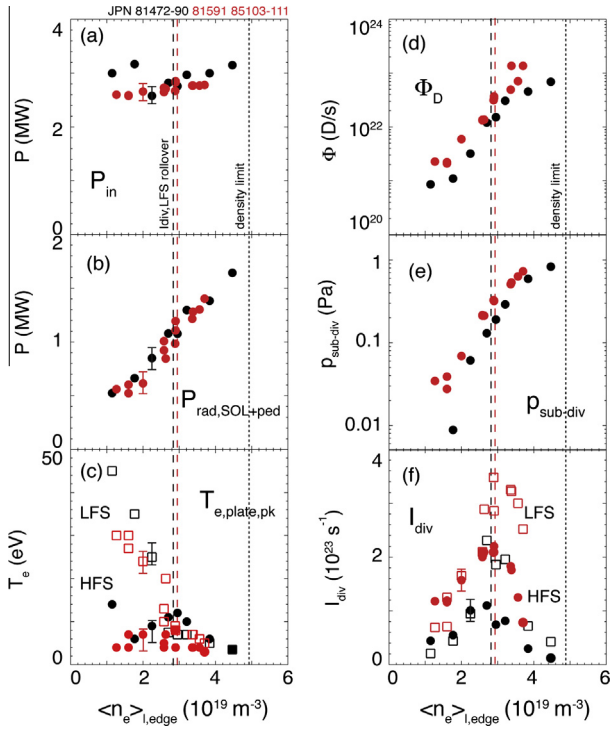

Fig. 2. Measured (a) total input power (P_{in}), (b) total radiated power in the SOL and pedestal region ($P_{rad,SOL+ped}$), (c) peak T_e in the near-separatrix region at the HFS (solid circles) and LFS (open squares), (d) total atomic deuterium input, (e) baratron sub-divertor pressure, and (f) total ion current to the HFS (closed circles) and LFS (open squares) plates as function of line-averaged density at the core edge. Black symbols refer to the HT configuration, red symbols to the VT configuration.

The peak T_e (and j_{sat}) were determined from the Langmuir probe profiles at the targets within a radial distance of ±2 cm from the separatrix, and chosen to avoid misstating T_e and j_{sat} at the separatrix due to the uncertainty of separatrix location. (Due to the brevity of this paper, the target profiles are not shown here.) The profile shapes T_e and j_{sat} were almost identical between the HT and the VT configuration, including the position of the peaks in these parameters with respect to the strike points. For nearly identical $\langle n_e\rangle_{l,edge}$ values, the magnitudes of T_e at the LFS plate are the same within 50% for the HT and VT configurations, while the peak values of j_{sat} at the LFS plate are identical in both configurations. Similar qualitative and quantitative observations were made for the profiles of T_e and j_{sat} at the HFS plate. Here, the peak in j_{sat} was measured twice as high in the VT than in the HT configuration for low and mid-range $\langle n_e\rangle_{l,edge}$ (see also Fig. 2f).

Rollover of the ion saturation current occurred at almost identical $\langle n_e\rangle_{l,edge}$ in the HT and VT configurations (Fig. 2f). Furthermore, the rollover occurred at the same $\langle n_e\rangle_{l,edge}$ at the HFS and LFS plates. Here, the profiles of j_{sat} are spatially integrated across the HFS and LFS plates to give the total current. Generally, $I_{div,LFS}$ was 1.5 to 2 times higher than $I_{div,HFS}$. The difference in I_{div} between the HT and VT configuration is due to slightly different profiles shapes of j_{sat}. In both configurations I_{div} decreased by up to an order of magnitude (data for HT only) for $\langle n_e\rangle_{l,edge}$ approaching the density limit. These observations in neutral beam-heated plasmas are consistent with those in ohmic plasmas [6]. On the other hand, these results are inconsistent with measurements in DIII-D [18], AUG [19] and even JET [20], suggesting that divertor geometry and plasma configuration playing a significant role.

In the L-mode plasmas the neutral pressure in the sub-divertor, $p_{sub-div}$, was a factor of 2 higher in the VT than in the HT configuration (Fig. 2e), consistent with previous observations of increased neutral divertor pressures in vertical versus horizontal configurations [5]. Correspondingly, to achieve the same $\langle n_e\rangle_{l,edge}$ in the VT configuration, approximately twice as much D_2 fuelling was required than in the HT configuration (Fig. 2d). In ohmic plasmas approximately 2–3 times higher fuelling rates were required in the VT configuration [6]. Whether this increase in $p_{sub-div}$, and thus higher pumping rates, in the VT configuration is due to direct pathway of neutrals from the gas injection system to the sub-divertor pumping plena could not be addressed within these studies. Previous studies of injecting methane into the LFS strike zone in a HT configuration in JET with the carbon wall, however, indicated that about 33% of the methane injected from the same gas module was pumped out of the vacuum directly without entering the plasma [21]. Hence, it is conceivable, albeit not directly proven, that a significant fraction of the injected deuterium is indeed pumped directly. This effect may be stronger in the VT configuration, since the gas injection module at the LFS base plate is adjacent to the LFS pumping plenum.

3. EDGE2D-EIRENE simulations of the plasma conditions and neutral dynamics in HT and VT configurations

Raising the fuelling and thus the separatrix density at the LFS midplane ($n_{e,sep,LFS-mp}$), while keeping the power across the core boundary constant (2.2 MW), EDGE2D-EIRENE simulations show qualitatively the same response of $P_{rad,SOL+ped}$, I_{div}, and $T_{e,plate,pk}$ as observed in the experiments (Fig. 3). The distinct drop of $T_{e,plate,pk}$ from about 20 eV to 2–3 eV as observed experimentally (Fig. 2c), however, not is reproduced by the simulations. The rollover of I_{div} is predicted to occur at about 10% lower $n_{e,sep,LFS-mp}$ in the VT than

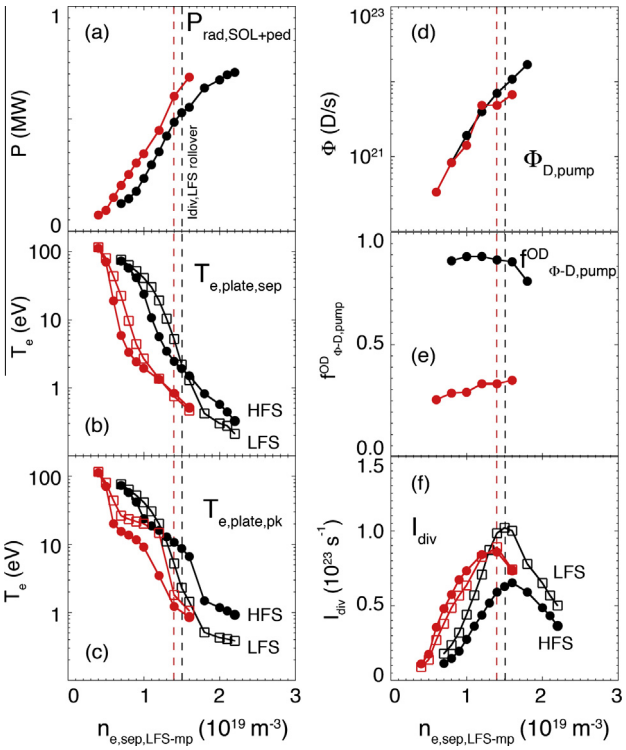

Fig. 3. EDGE2D-EIRENE predicted (a) total $P_{rad,SOL+ped}$, (b) T_e at the separatrix of HFS (closed circles) and LFS (open squares) plates, (c) peak T_e along the HFS (closed symbols) and LFS (open squares) plates, (d) total pumped atomic and molecular deuterium currents, (e) fraction of the total pump deuterium currents to the LFS pump surface, and (f) total ion current to the HFS (closed symbols) and LFS (open squares) plates as a function of separatrix density at the LFS midplane. Colour and symbol code as in Fig. 2. (For interpretation of the references to colour in this figure legend, the reader is referred to the web version of this article.)

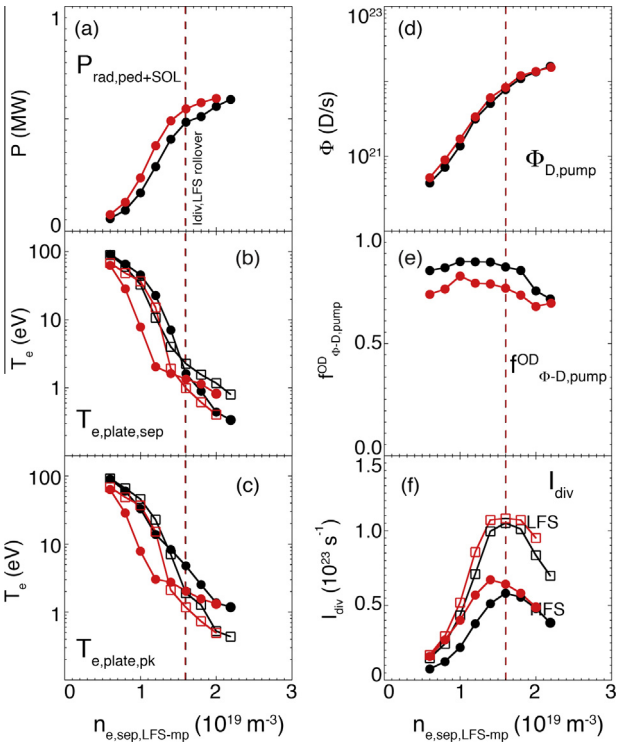

Fig. 4. EDGE2D-EIRENE predictions of same parameters as in Fig. 3 for pure-deuterium plasma in the HT configuration without (black) and with (red) cross-field drifts. (For interpretation of the references to colour in this figure legend, the reader is referred to the web version of this article.)

in the HT configuration, and takes place at the HFS and LFS plate at same $n_{e,sep,LFS-mp}$ (Fig. 3f). Assuming a 1-to-2 linear relationship between $n_{e,sep,LFS-mp}$ and $\langle n_e \rangle_{l,edge}$, as proposed previously by the authors [22], the rollover density of $I_{div,LFS}$ is predicted at the same density as observed in the experiment. At densities beyond the rollover, the predicted $I_{div,LFS}$ decreases by a factor of 2 in the HT configuration, while by 40% only in the VT configuration. Stable solutions could not be obtained for $n_{e,sep,LFS-mp}$ beyond those shown in Fig. 3. It is important to note that the rollover of $I_{div,LFS}$ is predicted to occur when $T_{e,LFS,pk}$ is as low as 2 eV, or lower.

The total radiated power in SOL and pedestal regions is predicted up to 30% higher in the VT than in the HT configuration (Fig. 3a): this is mainly due to stronger deuterium radiation in the divertor legs. Concomitantly, the predicted values for T_e at the HFS and LFS plates at the separatrix are significantly lower in the VT than in the HT configuration (Fig. 3b). For mid-range densities, i.e., $n_{e,sep,LFS-mp}$ in the range of 0.8 to 1.4×10^{19} m^{-3}, $T_{e,sep}$ is predicted to be a factor of 10 lower in the VT than in the HT configuration. For vertical targets, the predicted T_e profiles typically peak in the common SOL away from the separatrix (Fig. 3c). Therefore, the predicted $T_{e,plate,sep}$ better represent the measured $T_{e,plate,pk}$ than the predicted $T_{e,plate,pk}$. In general, the simulations reproduce what is conceptually considered for vertically inclined target configurations: reflection and release of deuterium atoms and molecules in the direction of the separatrix, leading to cooling of the plasma close to the separatrix and lower T_e. This behaviour is not observed in the measurements and thus needs to be further investigated in future experiments.

Including cross-field drifts in the simulations significantly reduces T_e at the HFS plate for a given $n_{e,sep,LFS-mp}$ (Fig. 4b and c). Or, in other words, plasma conditions of T_e of <2 eV are obtained at significantly lower $n_{e,sep,LFS-mp}$. The largest difference in $T_{e,HFS}$, is observed for the HT configuration, in which $T_e < 2$ eV conditions across the entire plate are obtained at $n_{e,sep,LFS-mp}$ half required for a no-drift case. These observations are consistent with previous investigations using EDGE2D-EIRENE [13] as well as other fluid codes, such as SOLPS [23] and UEDGE [24], underlining the impact of poloidal $E \times B$ drifts in the PFR increasing the plasma density in the HFS divertor leg. Concomitantly, the rollover of $I_{div,HFS}$ is predicted to occur at 15% lower $n_{e,sep,LFS-mp}$ (Fig. 4f), coinciding with $T_{e,HFS,pk}$ reaching 2 eV (Fig. 4c). However, the LFS plasma is less affected by the inclusion of drifts, and therefore, drifts not explain why the measured T_e profiles at the LFS plates are almost identical in the HT and VT configurations, and not so in the simulations. The radiation in the SOL slightly increases when including cross-field drifts due to increase radiation in the HFS divertor (Fig. 4a). Colder HFS divertor conditions also lead to an increase in deuterium removal at the divertor corners (Fig. 4e).

EDGE2D-EIRENE calculations of the neutral currents, including both deuterium atoms and molecules, indicate that the pump in the LFS divertor corner removes about 80% of the total injected deuterium in the HT configuration (Fig. 3e). In contrast, about 30% of the total injected deuterium is removed at the LFS corner in the VT configuration. The calculations are based on assuming equal albedos on both pumping surfaces. Considering the pathways for neutrals to reach the cryo pump and their associated conductances in the sub-divertor, the LFS pump ought to be more efficient (have a lower albedo) than the HFS pump. The simulations signify that even in vertical configurations, in which neutrals have to penetrate through the divertor plasma and PFR to reach the pump, this transport mechanism is sufficiently efficient to compete with the more ballistic reflection of particles into the LFS corner in a horizontal configuration. The total amount of deuterium

pumping is equal in the two configurations (Fig. 3d), and approximately a factor of 3 lower than what was observed experimentally. Hence, either the actual cryo pumping is higher in the experiment than assumed here, or other (divertor and main chamber) surfaces remove significant amount of deuterium, or deuterium gas is directly pumped from the gas injection module without entering the plasma. To address the former issue, in the HT configuration the pumping albedo of both pump surfaces was lowered from 0.94 to 0.5 to reach the experimental throughput, with little effect on the divertor plasma. In other studies [14, 20], albedos of down to 0.84 at the main wall were assumed to reproduce the experimental deuterium throughput.

To investigate the impact of by-pass leaks in the JET divertor structure on the plasma conditions at the LFS plate, an artificial pump surface is assumed in front of a gap between the two toroidal rows forming the vertical target at the LFS (Fig. 1, by-pass pump in green). The pump surface is directly adjacent to the gap and faces the plasma. Conceptually, such pumping ought to lead to increase in T_e provided the neutral density in front of the pump is sufficiently high. Lowering the albedo of the by-pass leak surface from 1.0 (no pumping) to 0.1 (90% pumping), however, shows that the predicted neutral density at the location of the pump surface is too small to impact the overall recycling at the LFS plate to reduce T_e. These studies were carried out for the VT configuration at $n_{e,sep,LFS\text{-}mp} = 1.0 \times 10^{19}$ m^{-3}, which showed the largest difference between HT and VT in the simulations. By imposing an albedo of 0.1 at the gap, the removed deuterium current reached 30% of the current going to both the HFS and LFS divertor pumps. Yet, $T_{e,LFS,sep}$ is predicted to remain at 3 eV.

Finally, EDGE2D-EIRENE predicts that the neutral leakage from the divertor into the main chamber is dominated via the HFS divertor in both the HT and VT configurations. With increasing $n_{e,sep,LFS\text{-}mp}$, and thus divertor degree of detachment, the leakage current at the HFS is predicted to increase from 1×10^{22} D/s to 4×10^{22} D/s. The magnitude of these currents is about 10–20% of the total ion currents to the plates, and of the same order as the pump currents. The LFS divertor is predicted to remain more opaque to neutrals, producing neutral leakage currents of the order 1×10^{22} D/s, and to become more transparent (about 2×) when the LFS divertor is fully detached. Hence, these EDGE2D-EIRENE simulations would suggest that JET is a neutral-tight divertor. Inclusion of cross-field drifts makes the HFS divertor more transparent to neutrals, as expected. For $n_{e,sep,LFS\text{-}mp}$ in the mid-density range, the HFS leakage current doubles to triples. Neutral leakage from the LFS divertor is less affected by the inclusion of drifts.

4. Summary

Similar plasma conditions and, in particular, almost an identical functional dependence on upstream density were measured with Langmuir probes in JET ohmic and neutral beam-heated L-mode plasmas in configurations with the LFS strike point on the LFS horizontal (HT) and on the LFS vertical (VT) divertor target plates. The HFS strike point was on the HFS vertical plate in both configurations. These measurements would suggest a very small impact of target plate inclination on ion current to and plasma temperature at the LFS divertor plate. The sub-divertor pressure, however, was observed being systematically higher in the VT configuration, by factors of 2 to 5, in turn, requiring higher D_2 fuelling rates to obtain the same core and SOL profiles at the LFS midplane. Our present hypothesis is that a significant fraction D_2 is pumped directly by the cryo pump from the LFS base plate gas injection module without entering the plasma.

The experimental results in L-mode plasmas may be summarised as follows:

- the plate-integrated ion currents, $I_{div,HFS}$ and $I_{div,LFS}$, have the same functional dependence with upstream density in the HT and VT configurations; the rollover of $I_{div,HFS}$ and $I_{div,LFS}$ occurred at a virtually identical upstream density,
- the peak values of j_{sat} at the HFS and LFS plates with upstream density are identical in the HT and VT configurations,
- the near-separatrix electron temperatures, $T_{e,pk,LFS}$, (and densities) at the LFS plate have the same functional with upstream density in the HT and VT configurations; the drop in electron temperature from 20 eV to 2–3 eV occurs at slightly lower upstream densities than the rollover of $I_{div,LFS}$,
- the sub-divertor pressure and the required D_2 fuelling is factors of 2 higher in the VT than in the HT configuration.

EDGE2D-EIRENE simulations of these plasmas also show the ion currents to the divertor plates to rollover into partial detachment at the same upstream density. However, significantly lower plasma temperatures at the separatrix on the LFS plate are predicted for the VT configuration at intermediate upstream densities. The impact of enhanced radial transport in the SOL on at high upstream density detachment was not yet investigated. It is not clear, however, whether such transport, and hence enhanced plasma-main chamber interaction, would be different in the HT and VT configurations.

The EDGE2D-EIRENE predictions for the L-mode plasmas may be summarised as follows:

- the predicted plate-integrated ion currents, $I_{div,HFS}$ and $I_{div,LFS}$, have the same functional dependence with upstream density in the HT and VT configurations; the predicted rollover of $I_{div,HFS}$ and $I_{div,LFS}$ occurs at a slightly (10–15%) lower upstream density ($n_{e,sep,LFS\text{-}mp}$) in the VT than the HT configuration,
- the near-separatrix electron temperature at the LFS plate, $T_{e,pk,LFS}$, is predicted to drop below 2 eV at 30% lower upstream density in the VT than in the HT configuration; this prediction is inconsistent with the experimental data,
- the simulations predict a continuous decrease in $T_{e,pk,LFS}$, and do not indicate a sharp reduction of $T_{e,pk,LFS}$ from 20 eV to 2 eV at intermediate upstream density as observed experimentally,
- inclusion of cross-field drifts in the simulations reduces $T_{e,pk}$ at the HFS plate, but not at the LFS plate, and thus cannot explain the discrepancy between the experiments and simulations for $T_{e,pk,LFS}$ in the VT configuration,
- assuming an additional pump surface at the tile gap on the LFS vertical target plate to mimic a by-pass leak does not raise $T_{e,pk,LFS}$, even when assuming a pump albedo of 0.1.

Acknowledgment

This work was supported by EURATOM and carried out within the framework of the European Fusion Development Agreement. The views and opinions expressed herein do not necessarily reflect those of the European Commission and those of the ITER organisation.

References

[1] A. Loarte et al., Nucl. Fusion 47 (2007) S203–S263.
[2] G. van Rooij et al., J. Nucl. Mater. 438 (2013) S42.
[3] B. Lipschultz et al., IAEA Fusion Energy Conference (1996), Proc. 16th Int. Conf. (Montreal, 1996), vol. 1, IAEA, Vienna, 1996.
[4] H.S. Bosch et al., Plasma Phys. Controlled Fusion 41 (1999) A401.
[5] A. Loarte et al., Nucl. Fusion 38 (1998) 331.
[6] M. Groth et al., 40th Conference on Plasma Physics, Espoo, Finland, July 1–5, 2013, P1.115.
[7] M. Groth et al., Nucl. Fusion 53 (2013) 093016.
[8] G.F. Matthews et al., J. Nucl. Mater. 438 (2013) S2.

[9] U. Kruezi et al., Rev. Sci. Instrum. 83 (2012) 10D728.
[10] D. Reiter et al., J. Nucl. Mater. 196–198 (1992) 80.
[11] R. Simonini et al., Contrib. Plasma Phys. 34 (1994) 368.
[12] S. Wiesen, EDGE2D-EIRENE code interface report, JET ITC-Report, <http://www.eirene.de/e2deir_report_30jun06.pdf>, 2006.
[13] A.V. Chankin et al., J. Nucl. Mater. 290–293 (2001) 518.
[14] V. Kotov et al., Plasma Phys. Controlled Fusion 50 (2008) 105012.
[15] S. Brezinsek et al., J. Nucl. Mater. 438 (2013) S303.
[16] A.G. Meigs et al., J. Nucl. Mater. 438 (2013) S607.
[17] A. Loarte et al., Plasma Phys. Controlled Fusion 43 (2001) R218.
[18] M. Groth et al., Plasma Phys. Controlled Fusion 53 (2011) 124017.
[19] M. Wischmeier et al., J. Nucl. Mater. 415 (2011) S523.
[20] C. Guillemaut et al., Nucl. Fusion 54 (2014) 903012.
[21] J. Likonen et al., Phys. Scr. T145 (2011) 014004.
[22] M. Groth et al., J. Nucl. Mater. 438 (2013) S175.
[23] D. Coster et al., Czech J. Phys. 48 (S2) (1998) 327.
[24] T.D. Rognlien et al., Phys. Plasma 6 (1999) 1851.